USE OF DIFFERENT FRICTION MODELS ON THE AUTOMOTIVE CLUTCH ENERGY SIMULATION DURING VEHICLE LAUNCH

Edson Luciano Duque, edson.duque@gm.com
Marco Antonio Barreto, marco.barreto@gm.com
GM Powertrain South America – São Caetano do Sul – SP – Brazil

Agenor de Toledo Fleury, agfleury@fei.edu.br
Centro Universitário da FEI – São Bernardo do Campo – SP – Brazil

Abstract. *The clutch system works basically as an interface between the engine and the vehicle. The engine provides power and torque in a given revolution while the vehicle launches. The slipping time is a critical moment for the clutch during this phase. Then, many studies have been done to predict the total slip time, and the related amount of energy during clutch engagement.*
Considerations about this energy are highly important in clutch capacity analysis, and some available studies evaluate several aspects that take place during the slipping phase, where simple or complex models represent all the dynamics involved in related systems.
Throughout a study case a proposed model based on Coulomb friction is compared to a static model found in the literature and to measurements done in a sample vehicle in order to check the accuracy of the model.
Besides to the Coulomb, the dynamic Stribeck friction model is evaluated to check the one which better matches to this situation. Numerical simulation results are presented and discussed for both cases.

Keywords*: clutch, simulation, friction models*

1. INTRODUCTION

Engine and transmission speeds have a considerable variation during vehicle start-up, mainly because of driver influence. A schematic representation is shown in Figure 1. During the launch phase, the driver has major influence in throttle and clutch pedals behavior, acting directly in the dynamics involved in the process.

Many models developed for clutch energy simulation can be found in the available literature, but few represent well all the dynamic aspects involved during vehicle start-up (Shaver, 1997; Szadkowski and Mcnerney, 1992; Szadkowski and Morford, 1992).

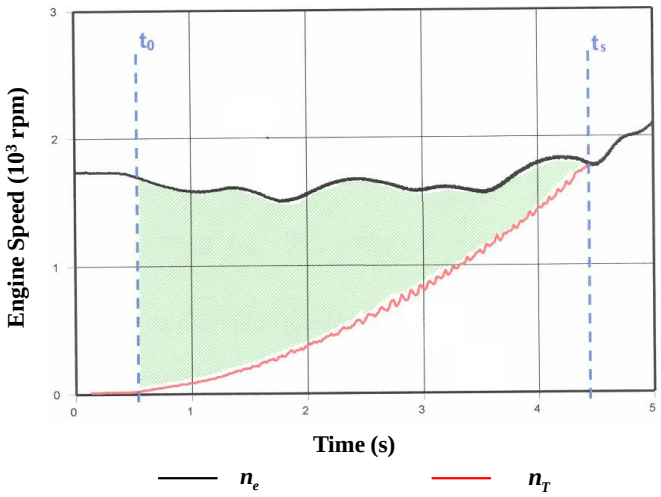

Figure 1. Representation of engine and transmission speeds during vehicle start-up
Source: Adapted from Duque (2010), p. 24

The total clutch energy Q generated during the launch represented by Figure 1 can be calculated as shown below (Shaver, 1997):

$$Q = \int_0^{t_s} T_c.\omega_r(t).dt \tag{1}$$

Where: $\omega_r(t) = \dot{\theta}_e - \dot{\theta}_T$, being $\dot{\theta}_e$ and $\dot{\theta}_T$ the engine and transmission angular velocities respectively, and T_c the generic torque generated by the clutch.

Static models consider only that maximum engine torque $T_e^{\max}$ in wide-open-throttle (WOT) condition, engine speed n_e and maximum clutch torque $T_c^{\max}$ as constants during slipping phase of the clutch providing a constant acceleration of transmission input shaft speed n_T (Shaver, 1997), which means that the driver profile is not taken into account, and the engine does not change its dynamics during a vehicle launch.

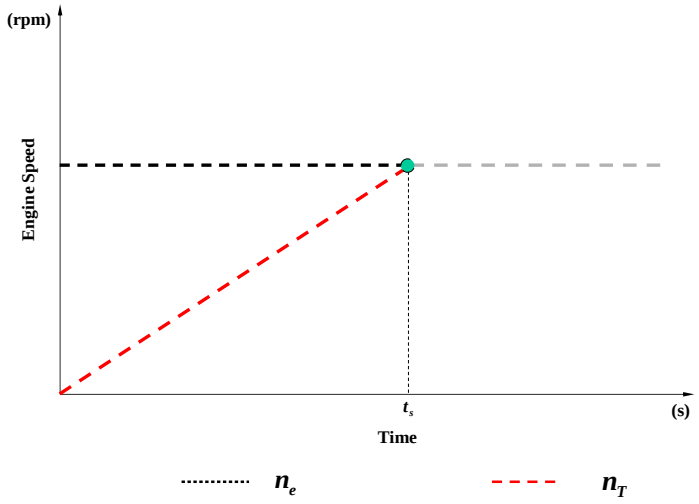

Figure 2. Simplified model output
Source: Adapted from Shaver (1997), p. 60

Considering the simplification seen in Shaver (1997), the slipping time t_s is:

$$t_s = \frac{\dot{\theta}_e.(I_V + I_T)}{T_c^{\max} - T_R} \tag{2}$$

Where I_V and I_T are the vehicle and transmission inertias respectively, and T_R is the resistance torque, calculated transporting total resistance force F_R of the vehicle to the transmission input shaft axis.

In this case, Q becomes:

$$Q = \frac{T_e^{\max}.\dot{\theta}_e.t_s}{2} \tag{3}$$

This oversimplified approach may lead to wrong assumptions and decisions about clutch system design in the early stages of a project, even considering that the results are used only for comparison between different vehicles or powertrain configurations.

Another point to be raised in such simplified models is that the engine mapping is not taken into consideration. The engine torque in partial-load condition has more weight during clutch slipping phase once maximum engine torque is hardly achieved during a vehicle start-up. Considering the more restrict vehicle emissions laws, engine response in mid revolutions has become more critical than ever.

As a consequence, only a more complex model should suit in this current condition, which the behavior of the driver, acting directly in the throttle and clutch pedals, and the characteristics in mid range of the engine are considered in the simulation.

2. MATH MODEL

The math model proposed in this paper is a hybrid version from the studies done by Duque (2005), and Szadkowski and Mcnerney (1992). This combined model will provide a basis to have the same model (and characteristics) to calculate heat generation, and transmission torsional vibration simulations.

The figure below shows the proposed model:

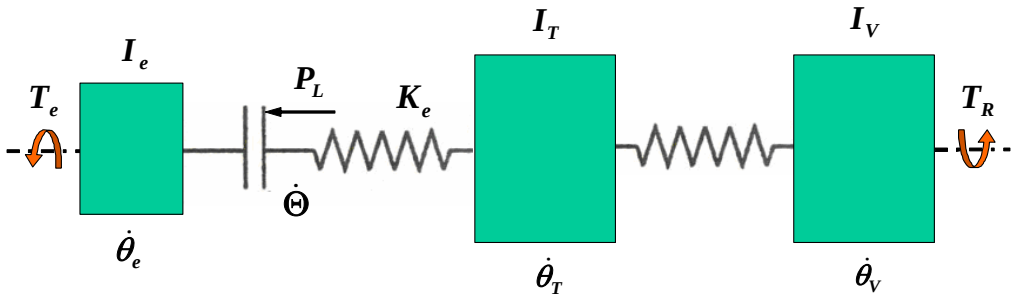

Figure 3. Proposed physical model
Source: Duque (2010), p. 97

All models presented are built in Matlab/Simulink R14 software, and the integration method chosen will be discussed later.

Regarding the friction torque generated by the clutch disc and cover assembly, at this moment the authors present the generic clutch torque T_c, which will be modeled according to friction models and discussed in the next items.

2.1. Friction models

Three friction models will be presented in the next items: Coulomb, combined Coulomb with viscous friction, and the model developed by Stribeck.

All models will be discussed in their general form and later adapted considering a clutch modeling approach.

2.1.1. Coulomb model

Also known as dry friction, Coulomb model is the most known friction model being used in lubricated and contact boundaries modeling. Although this model does not represent the contact behavior so well, it is used in several models to represent mechanical contacts in control systems modeling.

The friction Coulomb force F_C is proportional to the normal force N and to the friction coefficient μ_C.

$$F_C = \mu_C.N \tag{4}$$

It is noticed that F_C is independent of the relative velocity $\dot{x}$ between the surfaces under its action, see Figure 4a.

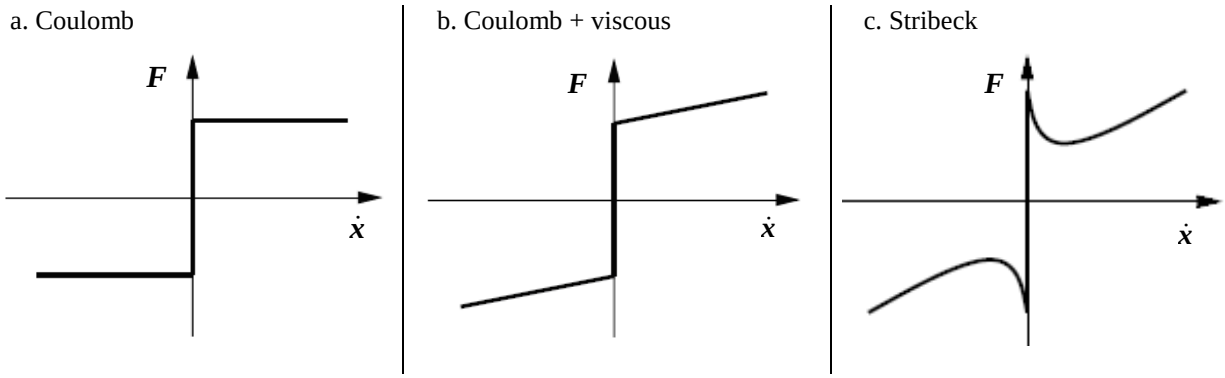

Figure 4. Representation of friction forces
Source: Adapted from Olsoon et al. (1997), p. 7

From Shaver (1997), applying the Coulomb model to clutch simulation, the clutch torque T_c^C is calculated based on the displacement of the pressure plate P_L, which, deforming the cushion springs, generates the normal load F_{cus} over the friction material (Duque, 2010). Being N_f the number of contact faces of the friction material of the clutch disc, T_c^C becomes:

$$T_c^C = \frac{2}{3}\mu_C.F_{cus}.N_f.\frac{(R_o^3 - R_i^3)}{(R_o^2 - R_i^2)} \tag{5}$$

2.1.2. Combined Coulomb and viscous friction model

Andersson et al. (2006) point that due to the non-linearity from Coulomb friction, the viscous friction model is normally applied (see Figure 4b). And, although, it provides an easier numerical solution, its physical representation is so reliable than the model developed by Coulomb:

$$F = k_v.\dot{x} \tag{6}$$

The viscous friction coefficient k_v allows expressing the dynamic system by linear differential equations, but it is not adequate to simulate a slipping situation.

Although the use of such combined models is convenient in oscillatory movements, they are not accurate to define the final position of a given body under action of low intensity forces, small displacements or movement reversals (Aberger and Otter, 2002; Andersson et al., 2006).

2.1.2. Stribeck model

Even dry contacts present similar behavior like lubricated surfaces, showing higher values of static friction compared to the ones when the body is moving. In lubricated surfaces, the friction force decreases with the increase of the slipping velocity until a stable condition is reached.

This behavior is more adequately modeled using the Stribeck assumptions (see Figure 4c) which lead to the following equation:

$$F = \left[F_C + (F_s - F_C).e^{-\left(\frac{|\dot{x}|}{v_s}\right)^i} \right].\mathrm{sgn}(\dot{x}) + k_v.\dot{x} \tag{7}$$

Here F_s is the maximum static friction force, v_S is the Stribeck velocity, and i is an exponent responsible for defining the shape of the curve. But, although this model has a good physical representation, covering fully both Coulomb and viscous models, still has the same difficulties during reversals.

Abberger and Otter (2002) rewrite Eq.(7) in function of friction coefficients, disregarding the viscous friction portion once a dry friction clutch is being analyzed:

$$\mu_{Str} = \mu_C + (\mu_{Est} - \mu_C).e^{-\left(\frac{\omega_r}{\omega_s}\right)^i} \tag{8}$$

Where T_c^{Est} is the friction torque calculated using the static coefficient μ_{Est} of the facing materials, ω_S is the Stribeck angular velocity and ω_r is the angular relative velocity between engine and clutch disc/transmission input shaft. Considering the same form of Eq.(5), T_c^{Str} can be also expressed in function of the normal force generated by cushion springs F_{cus}:

$$T_c^{Str} = \frac{2}{3}\mu_{Str}.F_{cus}.N_f.\frac{(R_o^3 - R_i^3)}{(R_o^2 - R_i^2)} \tag{9}$$

2.2. Engine model

Based on the model presented by Szadkowski and Morford (2002), the engine model is shown in the figure below, where the engine inertia I_e is accelerated by the engine torque T_e, and the clutch torque T_c counteracting the movement.

Considering the representation above, Szadkowski and Morford (1992) write the following equation for the engine:

$$\ddot{\theta}_e = \frac{T_e - T_c}{I_e} \tag{10}$$

Engine torque T_e depends on throttle position P_T and engine speed $\dot{\theta}_e$. Using an engine map containing these three parameters, a linear regression was done using the software Engineering Equation Solver (EES) v.7, generating a parametric second degree function. A surface was generated with this function and cross-checked against measured data from the sample engine, as seen in Figure 5 below:

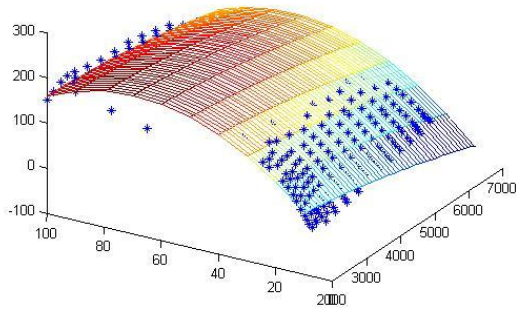

Figure 5. Measured data vs. proposed engine function surface

Other parameter of Eq.(10) to be calculated is the combined inertia I_e, and the assembly of Figure 6 has been considered in the model development.

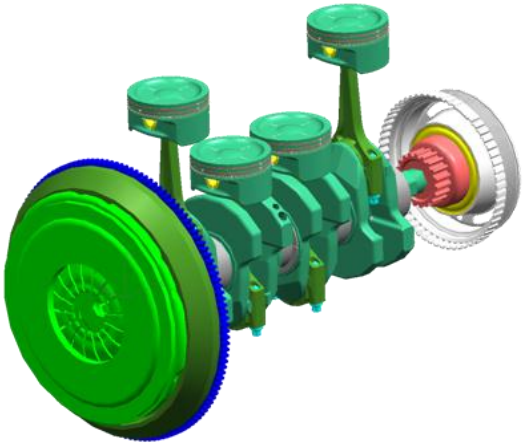

Figure 6. Crankshaft and pistons assembly

The inertia data are obtained from the math data for each component using the CAD software UniGraphics (UG) NX5, and then transported to the crankshaft rotation axis.

The inputs to the engine torque function block are the throttle position (%) during the launch and the engine speed n_e (rpm) with the initial condition set in the integration block as the same from vehicle measurements.

2.3. Clutch System Model

The configuration of the vehicle considered in this study is a cable-activated system, assembled with a push type diaphragm spring clutch cover, and clutch disc with torsional pre- and main dampers.

2.3.1. Clutch pedal and release system

The main characteristic considered is the total ratio between the clutch pedal and the fingers of the diaphragm spring measured in the vehicle. This relation can be seen in Figure 7:

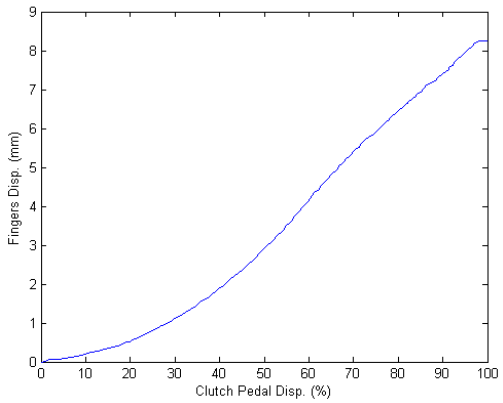

Figure 7. Pedal vs. Fingers displacement

This ratio should be measured from a similar vehicle with same installation components of the sample vehicle, but with a 1.0-liter flex fuel engine with a lighter clutch cover bearing load, which may represent a lower ratio when compared to the sample vehicle, equipped with a 1.4-liter flex fuel engine. Then, the curve above will be represented by a look-up table block in Simulink, and will be a baseline in the model, used as a convergence parameter for the simulation, if necessary. After the model is complete, some runs shall be made and their data correlated against launch measurements done in a, from now on, called sample vehicle, throttle and clutch pedal behavior measurements used as inputs to the model.

2.3.2. Clutch cover

For the clutch cover, the diaphragm spring finger versus plate displacement ratio is considered to translate the position of the fingers versus plate point, represented as a look-up table block in Simulink:

a.) Fingers vs. Plate displacement

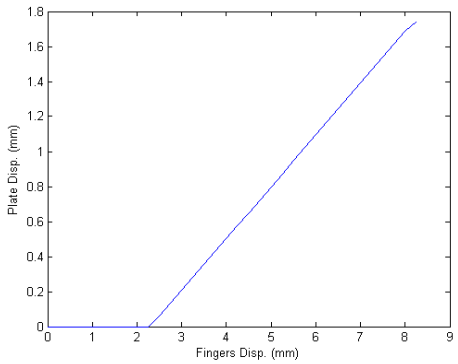

b.) Clamp Load

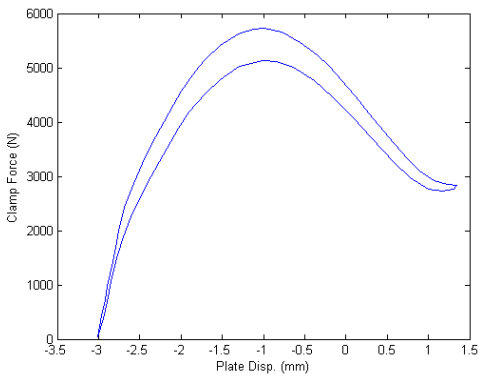

Figure 8. Clutch Cover Characteristic Curves

Another important characteristic of the cover is the clamp load curve, but here this curve is used to define the maximum clamp load that can be achieved with a new disc.

The maximum clamp load with a new disc is defined by merging the cushion spring load curve in the clamp force above. This will be demonstrated in the next item, concerning clutch disc.

2.3.3. Clutch disc

For the disc, the cushion spring curve has been measured and represented in a look-up table.

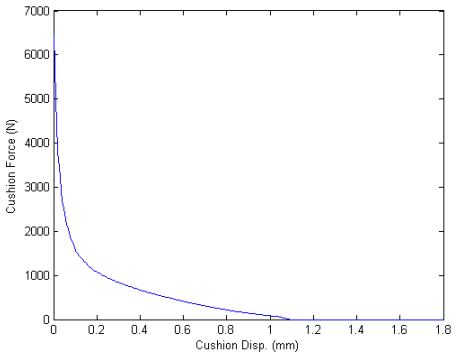

Figure 9. Cushion Force

Merging the cushion force from Figure 9 with the clamp load curve from Figure 8b, one should get the maximum normal force over the disc in a full engagement condition:

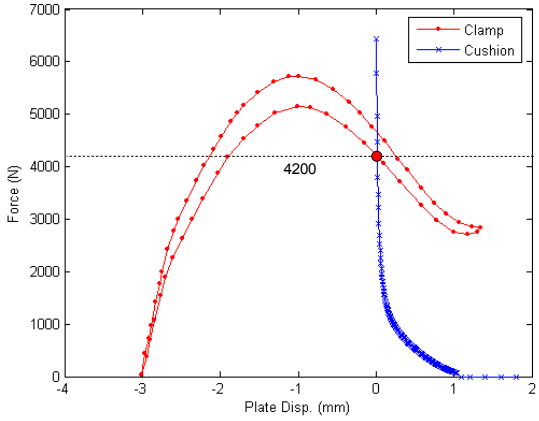

Figure 10. Maximum Clamp Force

This limitation will be represented in the simulation loop by a saturation block, thus avoiding any unreal behavior (overload) of the cushion force F_{cus} during engagement phase.

2.3.4. Clutch torque calculation

A function block is used to represent equations (5) and (9) in the simulation loop, using a measured clutch pedal schedule as input, the complete clutch model will provide the clutch torque behavior.

2.4. Driveline Model

As the sample vehicle is a front-wheel-driven, the driveline is composed basically by the half-shafts, which are represented by an equivalent stiffness coefficient K_D for a given gear ratio (Duque, 2005).

Considering that the vehicle launches in a straight line and no torque steering is detected, the same displacement is valid for both half-shafts. In this way, the half-shafts can be modeled as two springs acting in parallel, which gives:

$$k_{HS} = k_{HSr} + k_{HSl}$$

Transporting this combined stiffness to the input shaft of the transmission, K_D is calculated by:

$$K_D = \frac{k_{HS}}{\left(i_X . i_{Dif}\right)^2}$$

Where i_x is the ratio of a given gear and i_{Dif} is the differential ratio.

2.5. Transmission Model

The transmission is represented by its inertia I_T under the action of T_c and counteraction of the torque provided by the equivalent stiffness K_D and driveline damping C_D. From Newton's 2nd law:

$$\ddot{\theta}_T = \frac{T_c - K_D.(\theta_T - \theta_V) - C_D.(\dot{\theta}_T - \dot{\theta}_V)}{I_T} \tag{10}$$

And, being the transmission inertia per gear transported to the input shaft of the transmission (Duque, 2005).

2.6. Vehicle Model

Figure 11 below synthetizes the general assumptions made for the vehicle model in this work. It is considered that a vehicle of mass m_V is in a given slope, where it is accelerated by the tractive force F_{Tr} against a resistance force F_R.

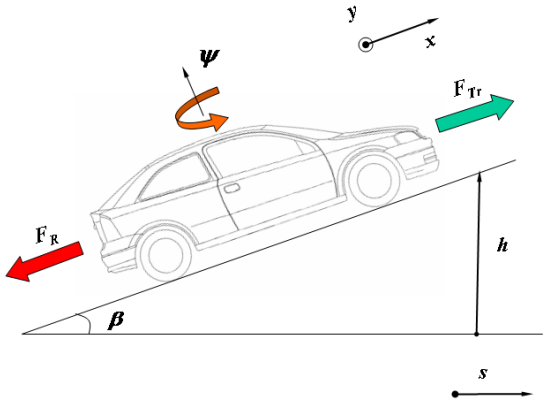

Figure 11. Vehicle representation

2.6.1.Vehicle inertia

Transporting this model to the input shaft of the transmission, equivalent vehicle model is composed by the equivalent inertia of the vehicle I_V, under action of K_D and C_D, and the counteraction of T_R.

Considering that the vehicle is not in a ramp, which means $\beta = 0°$, the following equation is obtained:

$$\ddot{\theta}_V = \frac{K_D.(\theta_T - \theta_V) + C_D.(\dot{\theta}_T - \dot{\theta}_V) - T_R}{I_V} \tag{11}$$

To calculate I_V, Duque (2005) uses the equation below:

$$I_{V_X} = m_V . R_D^2 . \frac{1}{\left(i_X . i_{Dif}\right)^2} \tag{12}$$

Where R_D is the dynamic radius of the tire, i_{Dif} the differential ratio, and i_X the ratio of a given gear.

2.6.2. Resistance force

A simple way to calculate F_R is to use the coast down coefficients of the vehicle measured through test procedure SAE J2263 (1996). Using this model with corrected coefficients, the resistance equation becomes:

$$F_R = f_0' + f_1'.x_V + f_2'.\dot{x}_V^2 \tag{13}$$

The resistance torque T_R is obtained transporting F_R to the input shaft of the transmission system:

$$T_R = \frac{1}{e}.\frac{R_D}{(i_X.i_{Dif})}.F_R \tag{14}$$

2.6.3. Vehicle/transmission block

Writing equations (10) and (11) in state-space format:

$$\dot{\mathbf{x}} = \mathbf{A}\mathbf{x} + \mathbf{B}\mathbf{u}$$

$$\begin{bmatrix} \dot{\theta}_T \\ \ddot{\theta}_T \\ \dot{\theta}_V \\ \ddot{\theta}_V \end{bmatrix} = \begin{bmatrix} 0 & 1 & 0 & 0 \\ -\frac{K_D}{I_T} & -\frac{C_D}{I_T} & \frac{K_D}{I_T} & \frac{C_D}{I_T} \\ 0 & 0 & 0 & 1 \\ \frac{K_D}{I_V} & \frac{C_D}{I_V} & -\frac{K_D}{I_V} & -\frac{C_D}{I_V} \end{bmatrix} \cdot \begin{bmatrix} \theta_T \\ \dot{\theta}_T \\ \theta_V \\ \dot{\theta}_V \end{bmatrix} + \begin{bmatrix} 0 & 0 \\ \frac{1}{I_T} & 0 \\ 0 & 0 \\ 0 & -\frac{1}{I_V} \end{bmatrix} \cdot \begin{bmatrix} T_c \\ T_R \end{bmatrix}$$

Once this is a system formed by linear equations, Simulink state-space block shall be used, considering T_c and T_R as inputs. Since the vehicle will start from rest, the initial condition vector is defined as:

$$X_0 = [0 \quad 0 \quad 0 \quad 0]^T$$

After these considerations, the model in Simulink is structured:

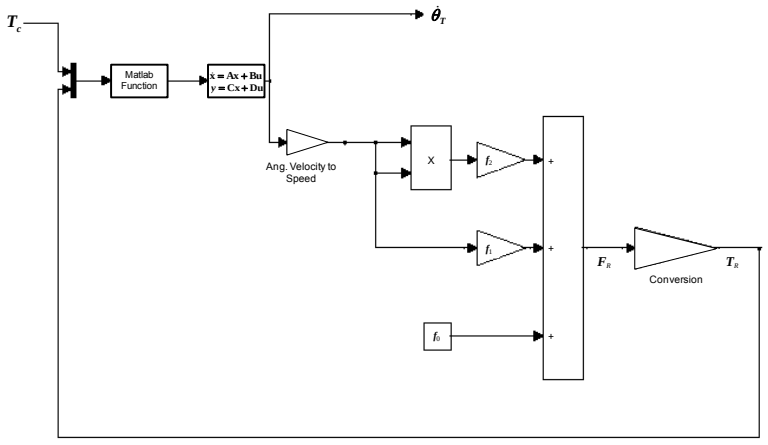

Figure 12. Transmission & Vehicle Model in Simulink

2.7. Choosing the integration algorithm

The integrators family of ordinary differential equation (ODE) from Matlab/Simulink provides a good number of algorithms for several types of problems: ode113, ode15s, ode23, ode23s, ode23t, ode23tb, and ode45. See details in Matsumoto (2004) and Shampine and Reichelt (2009).

The "first try" recommended by Matsumoto (2004) is ode45, which is an explicit Runge-Kutta (4,5) pair with local extrapolation developed by Dormand and Prince(1980), a.k.a. 7-stage RK5(4)7FM. Although this solver is considered one of the most efficient of this RK family, it may be too slow when used to solve stiff problems.

So, to check the stiffness of a given system, Dormand (1996) defines the stiffness ratio S :

$$S = \frac{\max|\Re(\lambda_k)|}{\min|\Re(\lambda_k)|}$$

Where λ_k are the eigenvalues of dynamic matrix $\mathbf{A}$ of the system. So, for large values of S the solver faces markedly different absolute stability requirements from extreme eigenvalues, leading to higher computational costs and time to get the solution done.

In the study case of this paper, a stiffness check will be done, and then the proper solver will be chosen.

3. STUDY CASE

Some launches have been measured in a sample vehicle, and throttle and clutch pedal schedules will now be used as inputs to the simulation model. The characteristics of the measured vehicle are shown in Table 1:

Table 1. Vehicle Data.

Mass	1150 kg	**1st gear ratio**	3.73
Dyn. Radius	0.284 m	**Final Drive ratio**	3.94
Coast Down (f_0', f_1', f_2')	175.9 N	**Trans. Inertia**	$1.12*10^{-3}$ kg.m^2
	-0.89 N/(km/h)	**Trans. Efficiency**	0.92
	0.54 N/(km/h)^2	**Clutch Diameters**	134 mm (inner)
Driveline Damping	5 N.m.rad/s		190 mm (outer)
Ramp	0%	**N. of facings**	2
Engine Inertia	0.15 kg.m^2	**Clutch friction coefficient**	0.27
Half-Shaft length	980.3 mm (R)	**Clutch Inertia**	0.022 kg.m^2 (cover)
	633.3 mm (L)		0.0039 kg.m^2 (disc)

To check the sensitivity of the model to vehicle mass variation, 300 kg was added to the vehicle and another sequence of measurements has been done. All simulation results are summarized in the next item.

With the data in Table 1, ratio S shows that the equations system proposed in the previous chapters is stiff which demands a solver that matches better to this type of condition. The integrator chosen is the ode23s, which, according to Matsumoto (2004), will improve simulation speed keeping numerical stability under control in this situation.

4. RESULTS

Launches have been performed in a sample vehicle and the comparison of measurements results to the proposed simulation model using both friction models, with and without the additional 300 kg load is shown in the sequence.

Coulomb

a.) Test mass

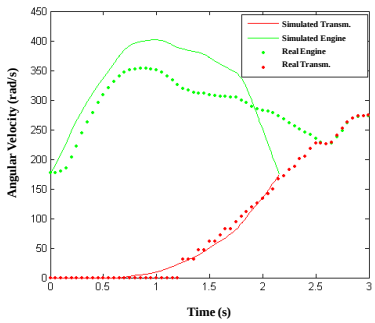

b.) With load (300 kg)

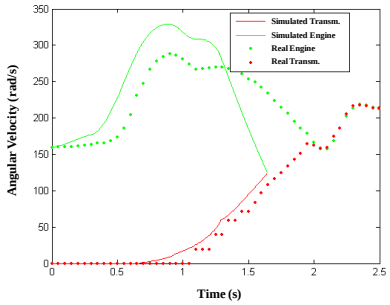

Stribeck

a.) Test mass

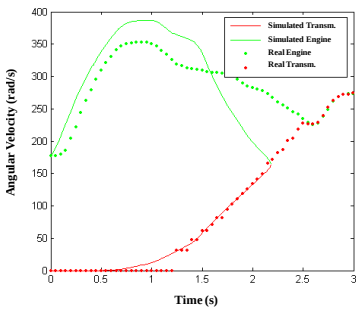

b.) With load (300 kg)

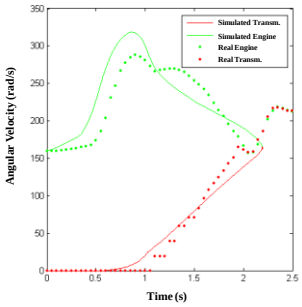

Figure 13. Engine and transmission speed behavior results

Comparing the simulations that consider the two friction models and using equations (2) and (3) for the simplified model presented by Shaver (1997), the following table has been prepared for synthesis purposes:

Table 2. Summary results table – all models, with and without load.

		Test Mass (1150 kg)	**Test Mass + 300 kg (1450 kg)**
Coulomb	t_s	**2.15 s**	**1.65 s**
	Q	27.85 kJ	19.85 kJ
Stribeck	t_s	**2.25 s**	**2.19 s**
	Q	26.98 kJ	24.41 kJ
Simplified	t_s	**0.97 s**	**1.12 s**
	Q	11.26 kJ	11.76 kJ
Measurements	t_s	**2.55 s**	**2 s**
	Q	29.81 kJ	27.78 kJ

5. CONCLUSIONS

Both proposed math models represent a step forwards in terms of powertrain dynamic behavior when compared to the simplified approach, showing better responsiveness to throttle and clutch pedal inputs. Although the model showed good feedback, the engine model presented poor response with the mass variation study which required higher

percentage of throttle. This condition led to "spikes" in engine speed in the beginning of the simulation, resulting in energy values not observed in the real vehicle (see Figure 14).

Checking the simulated engine torque versus the torque calculated by the engine control module (ECM) it can be noticed that differences are present in all revs range, and seems to be the reason of this difference, where seems that the real torque curve is delayed when compared to the simulated one.

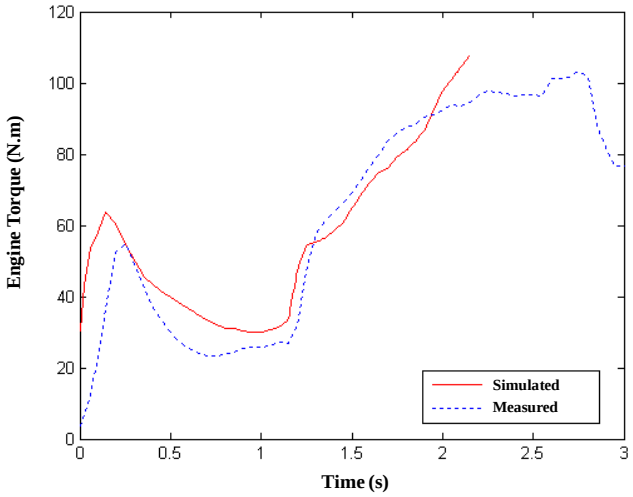

Figure 14. Engine torque simulated versus measured from ECM – Coulomb, no additional load

Checking the engine torque behavior to the input of the throttle schedule from the measurements, one obtains Figure 15:

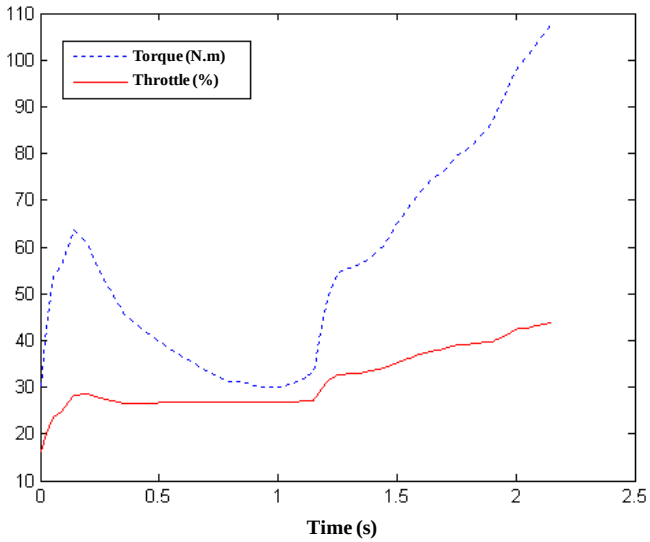

Figure 15. Simulated engine torque simulated versus throttle schedule

From this figure, one observes that the throttle opening percentage was in a range of 15% to 45%, which is within the correlation limits seen in Figure 5. In this way, it can be concluded that the problem is in the dynamic modeling of the engine, especially in the way chosen to represent the torque behavior with throttle and revolution inputs. This leads to an improvement of the engine model, maybe in the direction of the engine model suggested by Kiencke and Nielsen (2005) where the combustion data and engine friction are considered in the model. Following this idea, from the engine data available, the indicated mean effective pressure (IMEP) and the motoring torque of the sample engine are used to build a more robust model. This assumption may avoid the spikes found in the model proposed in this paper.

Another important point to be analyzed is the fact that for each start one will have a different throttle and clutch pedals schedule, mainly due to specific characteristics of different drivers. Deeper analyses are required in this front once is one of the uncertainties covered by the safety factor applied by most of vehicle manufactures. Having a better understanding of these input parameters with a statistical approach would improve the robustness of the model.

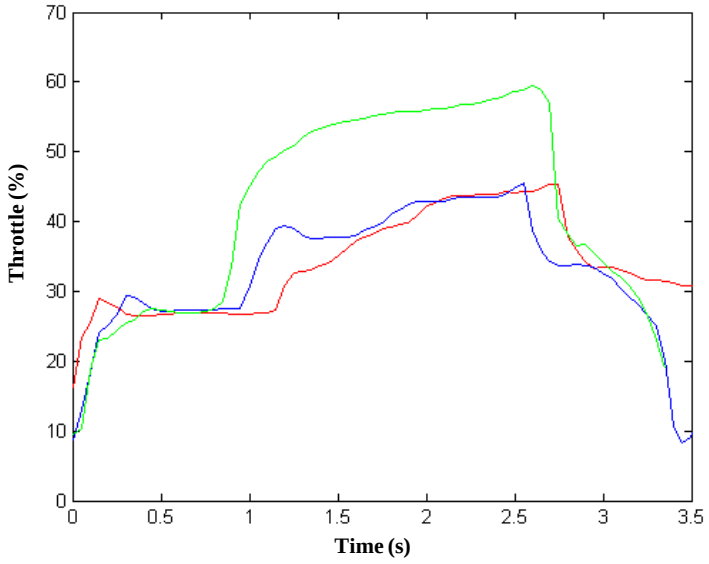

Figure 16. Comparison of throttle behavior in different launches – Coulomb without load

To improve this situation, Szadkowski and Mcnerney (1992) proposed a better launch logic. Their algorithm leads to a launch with a maximum allowed acceleration of the vehicle, limited by a no-kill condition for the engine, based on a given revolution (e.g. no lower than idle speed). The second part of this control verifies the longitudinal acceleration of the vehicle (no high peaks), which provides a no-jerk situation for the vehicle during the launch phase.

Another alternative is to use the proposal developed by Przybilla et al. (2011), where a Monte-Carlo simulation defines the driver profile taking into account the distribution of different driver behaviors, since a smoother to a more severe usage of throttle and clutch pedals in the vehicle launch.

Regarding the friction models, Coulomb model showed an acceptable result, but as Shaver (1997) said the friction behavior in the facing materials is highly dependent of relative velocity and temperature in the facing materials, and its static behavior does not provide the necessary flexibility to study this situation. Although presenting a better responsiveness than the simplified version, it can be seen in Table 2 that the Coulomb based model does not have a good correlation with the heavier situation.

The Stribeck model showed a good correlation in both load cases, regarding not only energy Q, but also with the slipping time t_s, mainly due to the higher flexibility inherent of this dynamic model.

Another alternative for future studies is the use of Lund-Grenoble (LuGre) friction in the clutch modeling, which combines the Dahl's model with the Stribeck's (Andersson et al., 2006). And, although this model is strongly indicated for simulating small displacements with reversals in control systems with friction, a detailed work done by Aberger and Otter (2002) presents an application of the LuGre model for the clutch torque calculation with good correlation, being a good alternative for the next studies.

6. ACKNOWLEDGEMENTS

The work presented here has been performed with support of Mr. Flavio Dias (M. Sc.), Mr. Daniel Rosa, Mr. Leandro Peres, and Mr. Rodrigo Augusto from GM Powertrain South America. Authors also acknowledges ZF Sachs do Brasil for vehicle measurements and technical discussions to improve the simulation models developed in this paper.

Finally, the third author acknowledges CNPq (grant 309329/2009-4) for financial support.

7. REFERENCES

Aberger, M.; Otter, 2002, M. "Modeling friction in Modelica with the Lund-Grenoble friction model". 2nd International Modelica Conference, Oberpfaffenhofen, Germany.

Andersson et al., 2006, "Friction models for sliding dry, boundary and mixed lubricated contacts". Sweden: Stockholm.

Bosch, R., 2005, "Manual de tecnologia automotiva: Robert Bosch", Ed. Edgard Blucher, São Paulo, Brazil.

Dormand, J. R.; Prince, P. J., 1980, "A family of embedded Runge-Kutta formulae". Journal of Computational and Applied Maths. Volume 6. Number 1, Cleveland, United Kingdom.

Dormand, J. R., 1996, "Numerical methods for differential equations: a computational approach", CRC Press, New York, United States of America.

Duque, E. L., 2005, "Efeito das vibrações torcionais do volante de motores na determinação do sistema de embreagem veicular", 175 p. Master Thesis (Automotive Engineering) – Escola Politécnica, Universidade de São Paulo, São Paulo, Brazil.

Duque, E. L., 2010, "Desenvolvimento de um modelo de simulação do acoplamento da embreagem durante a partida do veículo", 149 p. Master Thesis (Mechanical Engineering) – Centro Universitário da FEI, São Bernardo do Campo, Brazil.

Gillespie, T. D., 1992, "Fundamentals of vehicle dynamics", SAE, Warrendale, United States of America.

Kiencke, U.; Nielsen, L., 2005, "Automotive control systems: for engine, driveline, and vehicle", Ed. Springer, 2nd ed., Berlim, Germany.

Olsson, H. et al., 1997, "Friction models and friction compensation". Lund University, Lund, Sweden.

Przybilla, M. et al., 2011, "Combined simulation approach for dry clutch systems", SAE, Russelsheim, Germany (paper 2011-01-1232).

Matsumoto, E. Y., 2004, "Matlab 7: fundamentos", Ed. Érica, São Paulo, Brazil.

Society of Automotive Engineers, 1996, "SAE J2263: road load measurement using anemometry and coastdown techniques", SAE, Warrendale, United States of America.

Shampine, L. F.; Reichelt, M. W., 2009. "The Matlab ODE suite". 23 Jun. 2009, <http://www.cs.berkeley.edu/~wkahan/math128/ODEsuite.pdf>.

Shaver, R., 1997, "Manual transmission clutch systems", SAE, Warrendale, United States of America.

Szadkowski, A.; Mcnerney, G. J., 1992, "Clutch engagement simulation: engagement with throttle", SAE, Detroit, United States of America (paper 922483).

Szadkowski, A.; Morford, R. B., 1992, "Clutch engagement simulation: engagement without throttle", SAE, Detroit, United States of America (paper 920766).

6. RESPONSIBILITY NOTICE

The authors Edson Luciano Duque, Marco Antonio Barreto and Agenor de Toledo Fleury are the only responsible for the printed material included in this paper.